Oil Shale, 2014, Vol. 31, No. 1, pp. 91–101
doi: 10.3176/oil.2014.1.09
ISSN 0208-189X

OIL SHALE ASH BASED STONE FORMATION – HYDRATION, HARDENING DYNAMICS AND PHASE TRANSFORMATIONS

LEMBI-MERIKE RAADO[(a)*], REIN KUUSIK[(b)], TIINA HAIN[(a)], MAI UIBU[(b)], PEETER SOMELAR[(c)]

[(a)] Department of Building Production, Tallinn University of Technology, Ehitajate tee 5, 19086 Tallinn, Estonia
[(b)] Laboratory of Inorganic Materials, Tallinn University of Technology, Ehitajate tee 5, 19086 Tallinn, Estonia
[(c)] Department of Geology, University of Tartu, Ravila 14a, 50411 Tartu, Estonia

Abstract. *Combustion of low calorific fuel – oil shale – in industrial-scale pulverized firing and circulating fluidized bed combustion boilers produces large amounts of ash. Estonian oil shale ash is characterized by a high content of free CaO as compared to those listed in the European Standard EN 450. The main alternatives to oil shale ash utilization include its use as a lime replacement in mineral binders or as a constituent of Portland cement. The pulverized firing ash formed at 1400 °C has been effectively used as a second main constituent of Portland cement during the last fifty years. Further utilization of the low-temperature circulating fluidized bed ash (formed at 800 °C) depends on its composition and properties. Dust collecting systems of both boiler types consist of bottom dusters, cyclones and electrostatic precipitators. The corresponding ash types differ in specific surface area, grain size and mineral composition. The structure and composition of the dry ash and ash based stone were studied using chemical, XRD and SEM analysis. The results indicated that hydration type, as well as the setting and hardening course of the selected ash type are determined by the firing temperature of oil shale.*

Keywords: *types of oil shale ash, hydration, setting, hardening.*

1. Introduction

In Estonia, low calorific fuel oil shale (mineral content 55–65%) is primarily used for the production of electricity at two large power plants, the Baltic Power Plant and the Estonian Power Plant, based on pulverized firing (PF)

* Corresponding author: e-mail *lembi-merike.raado@ttu.ee*

and circulating fluidized bed (CFB) combustion technologies [1].The dust collecting systems of both boiler types consist of bottom dusters, cyclones (CA) and electrostatic precipitators (EF). The phase and chemical composition as well as the surface characteristics of different types of ashes [2] reflect the difference in duster types and combustion temperatures for the PF and CFB boilers, being higher in PF boilers (about 1400 °C) and lower in CFB units (about 800 °C). Changes in the firing technology have altered the mineral of the ash produced – the low temperature CFB ashes characterized by the lower content of silicates and aluminates and higher content of free oxides show predominantly pozzolanic hydration type and PF OSA has mostly hydraulic properties [3, 4]. The relationship between the composition of the solid fuel and its combustion temperature and the hydration type of the produced fly ash has been studied by many researchers [5–10].

Usage of various types of oil shale ash (OSA) as mineral binders depends on the course of hydration. Previous studies [3] have stated that coarse PF cyclone ash characterized by a high content of partly dead burned free CaO (about 20%) has predominantly non-hydraulic binding properties. Along the ash separation system, the content of free CaO and other free oxides decreases as the content of silicates and aluminates increases. This is also reflected on the binding properties of PF OSA from electrostatic precipitators, which has predominantly hydraulic properties with slightly revealed pozzolanic effect. The properties of high temperature PF OSA from electrostatic precipitators as a constituent of Portland cement are listed in the standard EVS 636:2002 [11]. Also, PF EF OSA has a unique property of reducing water demand of cement paste, increasing therefore the strength and durability properties of hardened concretes [12]. Ashes which do not meet the requirements of EVS 636:2002 have been used as lime replacements in agriculture and industry or stored as waste. Depending on the lime-containing component used in binders, including OSA, the OSA stone produced differs notably in the course of hardening and generated microstructure [3]. Ordinarily, the type and character of the hydration process determines the course of strength growth during hardening and the durability of hardened stone in water. Due to that, a wider utilization of coarse CA ash is still problematic and was therefore dealt with in this research.

The main goal of this research was to study the hydration type and binding characteristics of different kinds of OSA in correlation with changes in chemical and mineral composition. The study was focused on novel CFB OSA, the well-studied PF OSA from electrostatic precipitators was used for comparison. Another goal was to develop test methods to determine the binding properties and to predict the type and durability of ash stone. The rational utilization of OSA formed in boilers operating at different combustion technologies needs determination of its physical and chemical properties in combination with the methods used for testing binding properties of various binders such as lime and cement.

2. Materials and methods

OSA samples used in this investigation were collected from different points of the ash separation systems of PF and CFB boilers at the Estonian Power Plant. The high temperature PF OSA samples from cyclone and electrostatic precipitators (fields 1–3) were marked as 1ACA, 1AEF1, 1AEF2, and 1AEF3. The CFB samples from electrostatic precipitators (fields 1–4) were marked as 8AEF1, 8AEF2, 8AEF3, and 8AEF4. Particle shape, phase composition and some chemical and physical parameters of the tested OSA samples are shown in Figure 1, and Tables 1 and 2.

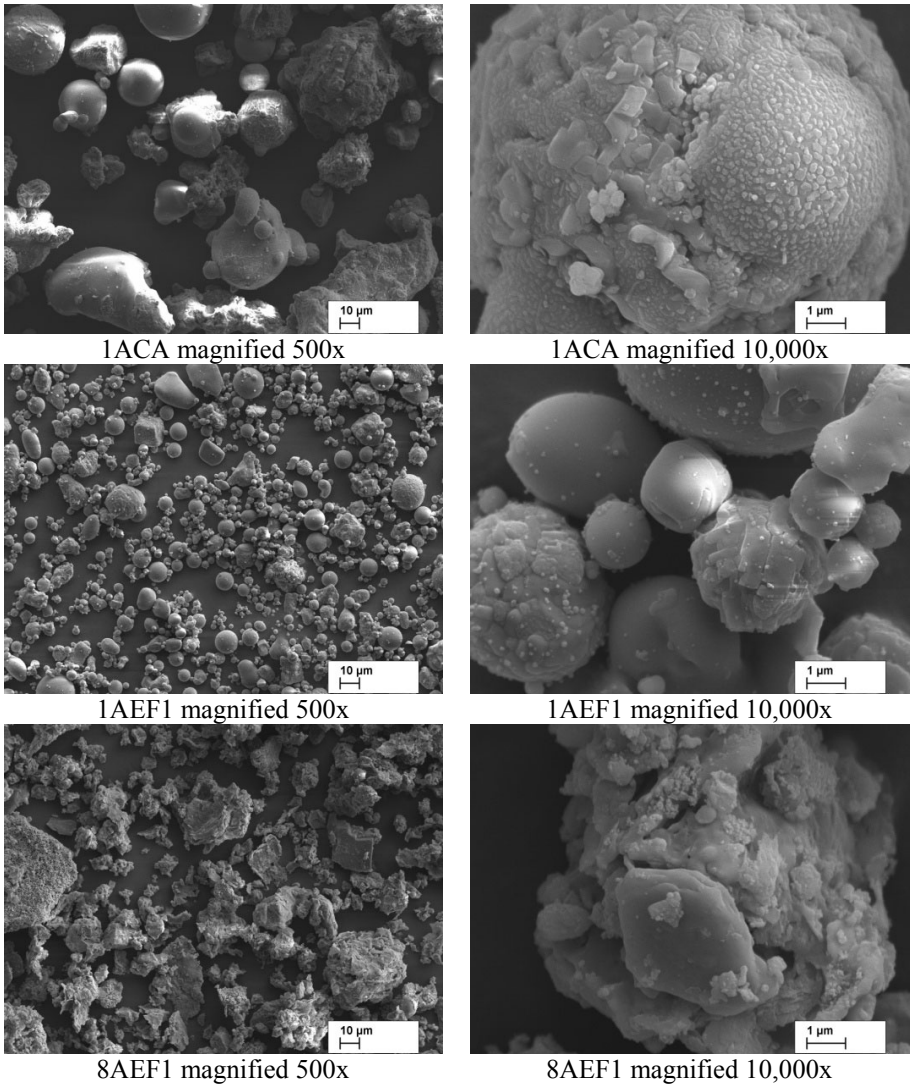

1ACA magnified 500x | 1ACA magnified 10,000x

1AEF1 magnified 500x | 1AEF1 magnified 10,000x

8AEF1 magnified 500x | 8AEF1 magnified 10,000x

Fig. 1. Grain shape and surface characteristics of tested OSA ashes.

Table 1. XRD analysis results of tested OSA types

Identified compound, phase	Content, %						
	1ACA	8AEF1	8AEF2	8AEF3	8AEF4	1AEF1	1AEF2
SiO_2	4.9	17.4	15.8	6.4	3.9	3.8	3.8
CaO	21.6	8.7	7.7	2.3	tr	11.3	11.4
$CaCO_3$	11.9	9.4	8.1	2.3	3.8	6.1	6.6
Fe_2O_3	1.7	4.9	5.0	3.0	3.9	1.3	1.4
MgO	3	2.8	2.5	1.8	1.0	1.6	1.8
$CaSO_4$	7.6	8.7	8.9	3.8	1.7	6.9	9.6
$2CaO{\cdot}SiO_2$	7.7	2.9	3.2	1.2	2.0	4.1	4.2
$4CaO{\cdot}Al_2O_3{\cdot}Fe_2O_3$	2.1	0	0	0	0	1.3	0
$CaO{\cdot}SiO_2$	0	0	0	0	1.1	0	0
$(Ca,Na)_2(Al,Mg,Fe^{2+})(Si_2O_7)$	1.9	2.5	2.9	2.5	1	1.3	0.7
$3CaO{\cdot}MgO{\cdot}2SiO_2$	2.9	1.6	1.3	0.9	0.8	0.9	1.7
Amorphous phase	32.2	23.6	28.6	67.4	73.8	59.7	57.1

Table 2. Characteristic properties of tested OSA types

Type of OSA	CaO_{fr}, %	SSA, m^2/kg
1ACA	23.8	116
1A EF1	14.1	314
8A EF1	10.8	217

The composition, specifications and conformity criteria for the production of mineral binders as well as the testing methods are regulated by various standards and norms today. The various methods used for testing specific properties of hydraulic binders, such as Portland cements [13, 14], or air binders, such as lime [15], substantially differ. The characteristics of OSA from electrostatic precipitators (1AEF and 8AEF) were tested using EN 196 [14] and also according to EVS-EN 459 [15] to determine slaking temperature and velocity, respectively. The conformity criteria for PF EF OSA as second main constituents of Portland cement are presented in EVS 636:2002 [11]. The specific surface area (SSA) of various OSA was tested by Blaine [14] (Table 2).

The binding properties of all OSA samples were tested in two stages, with hardened OSA pastes and mortars. Hardened for 28 days, ash stone specimens were used for BET and XRD analyses. Strength development was tested by EN 196 using the 4 x 4 x 16 cm prisms of a 1:3 OSA/sand mortar hardened for 7, 28 and 91 days.

The phase composition of OSA samples (Table 1) as well as hardened pastes was determined by quantitative XRD analysis in a Bruker D8 Advance diffractometer by Siroquant code using the full-profile Rietveld analysis. The content of free CaO was determined using chemical analysis [16].

The BET SSA of hardened ash pastes was determined using the KELVIN 1042 sorptometer (Costech Microanalytical SC, Estonia) (hardened pastes of 28 days were crushed to < 5 mm particles prior to analysis to go in the sample tube). The pore size distribution of hardened pastes was determined by Hg-porosimetry using the POREMASTER-60-17 porosimeter (Quantachrome Instruments, US).

3. Results and discussion

Phase analysis of PF and CFB ashes reveals the main differences between the tested materials (Table 1). The first field of the PF electrostatic precipitator catches up to 75%, the second field EF2, up to 8% of EF ashes. Consequently, the average mineralogical composition of EF ashes differs slightly from that of 1AEF1. CFB boilers have different dust gathering systems, but division of 8AEF ash by mass is almost the same. As compared to high temperature 1AEF ashes, low temperature 8AEF ashes have higher contents of free SiO_2, amorphous phase and non-decomposed $CaCO_3$, which consequently leads to the lower content of free CaO and calcium silicates. Also, according to Table 1, amorphous phase content has a tendency to increase along the dust collecting system (especially in 8AEF3-4).

The results of XRD-analysis do not agree with those of standard chemical analysis of CaO and $CaCO_3$ contents (Tables 1 and 2). Therefore, the further discussion of free CaO will be based on the results of chemical analysis (Table 2). These disagreements might be explained by the presence of multiple crystal forms of dead burnt CaO and also by the existence of the amorphous phase expressed as a background. Walenta and Füllmann [17] have reported highly reproducible quantification of sulphate, calcite and portlandite phases in cementitious materials, but an individual adaption method is needed for ashes, slags, etc.

Content of CaO_{fr} determines the hardening type of OSA. 1ACA is characterized by a high content of free CaO and a low specific surface area (Table 2). The listed properties of 1ACA, especially the high content of free CaO (23.8%), indicate air binding properties. The high firing temperature of PF boilers causes not only decomposition of limestone, formation of calcium silicates and aluminates, but also dead burning of free CaO, which leads to the formation of larger size crystals and decreased hydration reactivity. Hydration reactivity could be characterized by slaking rate and temperature (Fig. 2). To examine the slaking properties of free CaO containing ashes, the calculation method [15] had to be modified using a 100% hydration of the tested ash.

Slaking curves depict differences in the hydration type of the tested OSA samples (Fig. 2). 1ACA with the highest CaO content (23.8 %, Table 2) reaches maximum temperature (up to 40 ^{o}C) in 8 hours. Substantial differences can be observed during the same time period in the case of electrostatic precipitator ashes 8AEF1 and 1AEF1:

– The 1AEF1 delayed slaking or/and increase of hydration temperature (up to 48 °C) take place after > 33 hours.
– The initial moderate temperature rise (up to 32 °C) of low temperature 8AEF1 (CaO_{fr} = 10.8%; SSA = 217 m^2/kg, Table 2) was followed by an obvious decrease. Differences in the hydration type, as mentioned above, are clearly reflected on strength development (Table 3):
– 1ACA characterized by a high CaO content shows a very slow strength development as a typical air binder. The prisms had no compressive strength after 7 days of hardening. The compressive strength reached about 2 and 5 N/mm^2 after 28 and 91 days, respectively.
  The high temperature 1AEF1, characterized by the free CaO content of 14.1% and free SiO_2 content of 4.0%, as well as low water demand, has hydraulic binding properties. The compressive strength of 1AEF1 prisms reached 8.3 N/mm^2 and 22.8 N/mm^2 after 28 and 91 days, respectively.
– The low temperature 8AEF1, with the free CaO content of about 10.8% and free SiO_2 content of about 17.4%, has a high water demand as a typical pozzolana and its strength development differs notably from that of 1AEF1: in 7 up to 28 days of hardening, 8AEF1 and 1AEF1 prisms had an analogical strength development. Then the strength development ceased and after 91 days of hardening, the compressive strength of 8AEF1 prisms reached 8.8 N/mm^2.

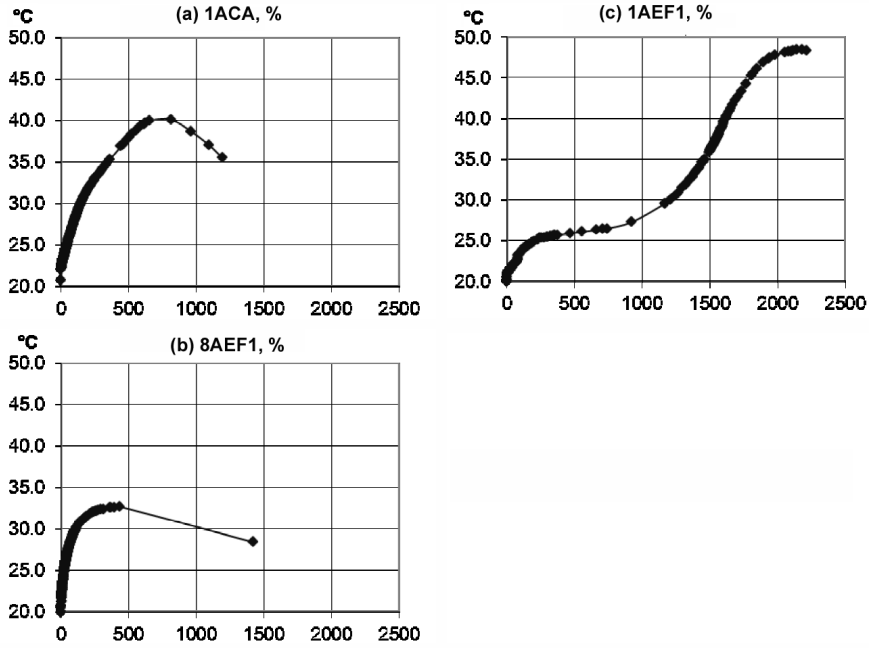

Fig. 2. Hydration heat curves of tested OSA (x –axis time of hydration in minutes).

Table 3. Compressive and flexural strength of OSA mortars

Type of OSA	Water: OSA ratio	Flexural strength, N/mm^2			Compressive strength, N/mm^2		
		7 d	28 d	91 d	7 d	28 d	91 d
1AEF1	0.37	0.9	1.4	4.4	4.3	8.3	22.8
8AEF1	0.78	1.6	1.8	2.6	4.7	7.0	8.8
1ACA	0.6	–	0.7	2.2	–	2.1	5.3

Colloidal hydration products of calcium silicates (CSH) have a diminishing effect on the capillary pore diameter (Fig. 3 and Table 4). Such a phenomenon decreases capillary pore volume. OSA based pastes (hardened for 28 days) were tested for BET SSA as well as for total pore volume and pore size distribution to identify the further durability risks like cracking and capillary water suction. The SSA of hardened pastes of 1AEF1 and 8AEF1 was 4.4–5.6 m^2/g and 8.2–9.7 m^2/g, respectively (Table 4). Substantial increase in porosity as well as average pore diameter was identified in 1ACA based pastes: total pore volume was 0.1868 mm^3/g and size of d_{mean} was 0.0828 μm. The measured d_{median} 11.68 μm suggests possible gaps in the examined hardened stone.

Figure 3 shows the pore size distribution of OSA based hardened pastes. 1ACA based pastes are characterized by the highest volume of capillary pores with a diameter ≥ 10 μm. In contrast, 1AEF1 based pastes have the lowest content of large capillary pores. The water demand of the binder,

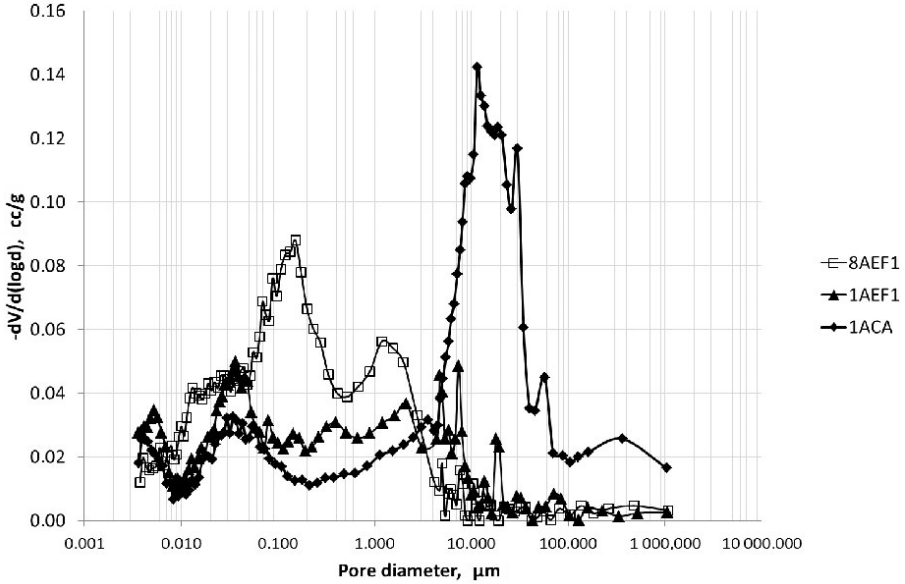

Fig. 3. Pore size distribution of OSA based hardened pastes.

Table 4. Pore characteristics of OSA pastes

Type of OSA	BET SSA, m^2/g (KELVIN 1042)	Total pore volume, mm^3/g	D_{mean}, μm	D_{median}, μm (by volume)
1AEF1	4.44-5.04	0.1053	0.0319	0.2905
8AEF1	8.17-9.75	0.1493	0.0490	0.1684
1ACA	4.27-5.28	0.1868	0.0828	11.68

which is mainly connected to the SSA of binders and presence of free CaO and SiO_2, has a decisive impact on the volume of capillary pores: the higher the water demand, the higher the volume of large capillary pores.

Part of the mixing water was expended on the hydration reaction of free CaO, which explains the high water demand of 1ACA, characterized by the highest free CaO content (23.8%) and the lowest SSA (116 m^2/kg) (Tables 2 and 3, Fig. 2a). It can be concluded that the hardening process of 1ACA is influenced by the temperature expansion and increased water demand, which leads to the genesis of large capillary pores.

Table 3 shows extremely high water demand also with CFB OSA 8AEF1. The low temperature ash from CFB boiler 8AEF1 has a low SSA (217 m^2/kg) combined with low hydration temperature. The main reason for high water demand is probably connected to the high free SiO_2 content (17.4%). Free SiO_2 reacts with free CaO and water, forming calcium silicate hydrate gel, which fills large capillary pores and decreases the volume of over 10 μm sized pores (Fig. 3). Pore structure characteristics have a direct impact on the permeability of ash stone [4, 6].

The high temperature 1AEF1 is characterized by a medium free CaO content (14.1%) and SSA (314 m^2/kg), but also low hydration temperature and low free SiO_2 content. The low water demand reported by Kikas [12] is due to the spherical form of 1AEF1 particles covered with a vitrified phase. Delayed temperature rise in Figure 2c indicates the hydration process of calcium silicates and aluminates.

The binder characteristics also include initial and final setting time. The period during which the paste starts to keep shape is determined by the initial setting time. The period during which the thickened paste is able to meet the stress from outside forces is fixed by the final setting time. The initial setting time of common Portland cement pastes is about > 45–75 min. The initial setting time of the tested OSA in Table 5 lies between 90 and 115 minutes and the final setting time is over 460 min with 8AEF1, which indicates the formation of calcium silicate hydrates.

Figure 4 shows changes in the content of characteristic compounds during the hydration, setting and hardening processes:

- obvious decrease in $Ca(OH)_2$ and SiO_2 contents in 8AEF1 pastes as compared to 1AEF1 pastes;
- ettringite formation in 8AEF pastes is hindered by the lack of $Ca(OH)_2$ needed for stabilization of ettringite crystals;
- the highest content of $Ca(OH)_2$ occurs in the hardened 1ACA paste.

Table 5. Setting time of OSA pastes

Type of OSA	SSA, m^2/kg	Water–OSA ratio for standard consistency	Initial setting time, min	Final setting time, min
8AEF1	217	0.71	90	460
1ACA	116	0.36	115	145
1A EF1	314	0.24	95	220

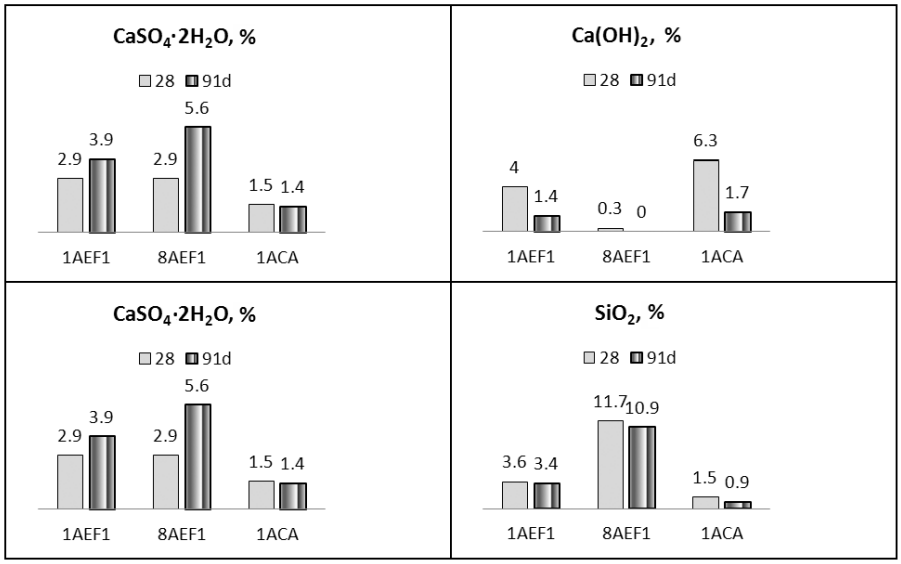

Fig. 4. Content of characteristic compounds and phases in the ash stone hardened for 28 and 91 days (XRD).

4. Conclusions

The high content of free CaO causes domination of quick lime-type hydration and slow rate of hardening. Co-phenomena of this process include significant expansion caused by differences in mole volume, hydration heat and low initial compressive strength of the OSA stone formed. As a result, the hardening process of cyclone ashes (1ACA) is characterized by increased water demand, which leads to low compressive strength, porous structure and unsatisfactory soundness of the formed ash stone.

OSA from high temperature PF electrostatic precipitators (1AEF1) is distinguished by decreased water demand. The hydration process includes ettringite formation due to a sufficient amount of $Ca(OH)_2$, followed by hydraulic reactions of calcium silicates and water. The ash stone formed is characterized by high compressive strength and small-sized capillary pores, which refer to its usability as a second main constituent of Portland cement.

OSA from CFB electrostatic precipitators (8AEF1) differs from PF ashes in high free SiO_2 content. The hydration type is mostly pozzolanic, characterized by increased water demand. Free SiO_2 reacts with free CaO and water, forming calcium silicate hydrate gel. Gel products fill large capillary pores and the volume of over 10 μm sized pores decreases. The hardening processes of CFB OSA and PF ashes develop during the first 28 days almost the same compressive strength, but the subsequent hydraulic hardening is hindered due to the lack of calcium silicates and aluminates.

Decreased capillary pore diameter and volume of CFB stone could indicate possible increased water resistance of CFB concrete, but it could also cause decreased resistance in conditions of the alternate wetting-drying.

Usage of pozzolanic ashes for concrete production requires further optimization of the composition of composites as well as their durability and hardening conditions.

Acknowledgements

The authors express their gratitude to Dr. Valdek Mikli for performing SEM analysis. This study was supported by the Estonian Research Council Targeted Financing Projects SF0690001s09 and SF0140082s08 and by the Archimedes project 3.2.0501. 10.0002 Basis for new application fields for solid wastes from oil shale combustion "Ash" (Supporting research and development in energy technologies) 2011–2014.

REFERENCES

1. Ots, A. *Oil Shale Fuel Combustion*. Tallinn, 2006.
2. Kuusik, R., Uibu, M., Kirsimäe, K. Characterization of oil shale ashes formed at industrial-scale CFBC boilers. *Oil Shale,* 2005, **22**(4), 407–420.
3. Raado, L.-M., Nurm, V. Properties of fluidized bed burnt oil shale ashes. In: *Proceedings of European Symposium of Service Life and Serviceability of Concrete Structures ESCS-2006* (Sarja, A., ed.). Espoo, 2006, 200–205.
4. Raado, L.-M., Tuisk, T., Rosenberg, M., Hain, T. Durability behavior of Portland burnt oil shale cement concrete. *Oil Shale*, 2011, **28**(4), 507–515.
5. Matcshei, T., Lothenbach, B., Glasser, F.P. The role of calcium carbonate in cement hydration. *Cement Concrete Res.*, 2007, **37**(4), 551–558.
6. Sakai, E., Miyahara, S., Ohsawa, S., Lee, S.-H., Daimon, M. Hydration of fly ash cement. *Cement Concrete Res.*, 2005, **35,** 1135–1140.
7. Marsh, B. K., Day, R. L., Bonner, D. G. Pore structure characteristics affecting the permeability of cement paste containing fly ash. *Cement Concrete Res.*, 1985, **15**(6), 1027–1038.
8. Hanehara, S., Tomosawa, F., Kobayakawa, M., Hwang, K. Effects of water/powder ratio, mixing ratio of fly ash, and curing temperature on pozzolanic reaction of fly ash in cement paste. *Cement Concrete Res*., 2001, **31**(1), 31–39.

9. Zhang, Y. M., Sun, W., Yan, H. D. Hydration of high-volume fly ash cement pastes. *Cement Concrete Comp.*, 2000, **22**(6), 445–452.
10. Marsh, B. K., Day, R. L. Pozzolanic and cementitious reactions of fly ash in blended cement pastes. *Cement Concrete Res.*, 1988, **18**(2), 301–310.
11. EVS 636:2002 Burnt oil shale for production Portland burnt oil shale cement, Portland composite and masonry cement.
12. Kikas, W. Composition and binder properties of Estonian kukersite oil shale ash. *Zement-Kalk-Gips International*, 1997, No. 2**,** 112–126.
13. EVS-EN 197-1:2011 Cement. Part 1: Composition, specifications and conformity criteria for common cements.
14. EN 196 Part: 1, 2, 3, 5, 6, 21. Methods of testing cement.
15. EVS-EN 459-2:2010 Building lime. Test methods.
16. EVS-EN 451-1:2004 Method of testing fly ash. Part 1: Determination of free calcium oxide content.
17. Walenta, G., Füllmann, T. Advances in quantitative XRD analysis for clinker, cements, and cementitious additions. In: *Advances in X-ray Analysis*, JCPDS, 2004, **47**, 287–295.

Presented by J. Hilger
Received March 22, 2013